

Carbon black as low-cost alternative for electrochemical sensing of phenolic compounds

Mailis M. Lounasvuori*, David Kelly and John S. Foord

Department of Chemistry, University of Oxford, Mansfield Road, Oxford OX1 3TA, UK

Abstract

Due to the toxicity and widespread presence of phenolic compounds in the environment, their accurate detection and monitoring is of great importance. The aim of this work was to find a viable low-cost alternative to expensive carbon nanomaterials such as carbon nanotubes and graphene. Carbon black, a conductive carbon nanomaterial that is produced in bulk quantities and is therefore cheap and readily available, was dropcoated onto glassy carbon electrode and used as electrochemical sensor to detect three phenolic compounds, catechol, p-cresol and p-nitrophenol. Compared to bare glassy carbon, the carbon black-modified electrode exhibited greatly enhanced current densities and lower oxidation potentials for all three phenols.

Calibration curves of catechol and p-cresol showed good linear response with concentration in the micromolar range, and detection limits of 41 and 63 nM were found for catechol and p-cresol, respectively. These results demonstrate the potential of carbon black as a low-cost, high-performance material for electrochemical sensing applications.

1 Introduction

Phenol and its derivatives are used as raw materials in a wide range of industrial activities, such as the production of herbicides, pesticides, and plastics [1-2]. Phenolic compounds are toxic [3] and can bioaccumulate in the environment [4-7]. Therefore, levels of phenols, including catechol, p-cresol, and p-nitrophenol, are monitored by environmental agencies within the EU [8] and USA [9]. The most commonly used methods for monitoring phenol

* Corresponding author. Tel: +44 18652 75630. Email: mailis.lounasvuori@chem.ox.ac.uk (Mailis Lounasvuori)

levels in environmental samples require time-consuming chromatographic separation prior to detection [10-14] with expensive, non-portable equipment [15] leading to long sampling times and high cost [16]. Development of a simple, low-cost, real-time analysis method is therefore desirable.

Electrochemical techniques are attractive due to their sensitivity, experimental simplicity, and low cost [17-18]. Different carbon nanomaterials have recently been used to construct electrochemical sensors, including carbon nanocages [19], carbon nanotubes [20] and functionalised carbon nanotubes [21-22]. The large surface area and excellent electron transport properties of these carbon nanomaterials enable electrochemical detection of phenolic compounds with high sensitivity and high selectivity. However, carbon nanocages and nanotubes are relatively expensive to synthesise and not readily available compared to carbon black (CB), which is cost-effective at ca. €1/kg [23] and produced in large quantities. CB-based electrochemical sensors have already been employed in the detection of catechol, gallic acid, caffeic acid and tyrosol [23-24]. Here, we report on the use of CB in electrochemical detection of catechol, *p*-nitrophenol and *p*-cresol (Figure 1) in aqueous solution. We compare the performance of bare glassy carbon electrode (GCE) to that of CB-modified GCE, focusing on sensitivity and the ability to detect low concentrations of phenols. We go on to demonstrate the feasibility of CB-modified GCE sensor in the quantification of catechol and *p*-cresol.

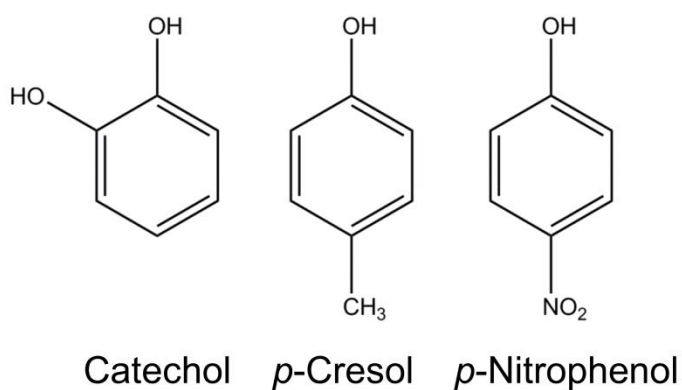


Figure 1: Chemical structures of the investigated phenolic compounds.

2 Experimental

Electrochemical experiments were performed with a μ -Autolab potentiostat/galvanostat (Ecochemie, NL) in a three-electrode setup with Ag/AgCl (1 M KCl) and Pt wire as reference and counter electrodes, respectively. GCE of diameter 3 mm (BASi, US) was used as the working electrode, and current densities of both bare and modified electrodes are calculated based on the geometric area of the GCE. The working electrode was polished using a felt pad and 1 μ m and 0.05 μ m alumina abrasive, then characterised using cyclic voltammetry (CV). A standard solution of 2 mM potassium ferricyanide, $K_3Fe(CN)_6$, was chosen as a reliable, readily available, quasi-reversible redox couple with which to characterise electrodes. Several CV scans were obtained at scan rates between 10 and 100 $mV s^{-1}$ in both blank 0.1 M phosphate buffer solution (PBS) at pH 7 and PBS containing 2 mM $K_3Fe(CN)_6$.

To prepare a CB- modified GCE, a suspension of Monarch 430 CB (Cabot Corporation, US) was prepared in water at a concentration of 1 $mg ml^{-1}$, drop-cast onto the GCE, allowed to dry, and the resultant coating inspected for even coverage. This surface-modified CB-GCE was characterised in the same way as above.

Initial detection of catechol, p-cresol, and p-nitrophenol was carried out by CV. The working electrode was immersed in the phenolic solution for 30 seconds, at which point a CV scan was obtained at a scan rate of 50 $mV s^{-1}$.

Differential pulse voltammetry (DPV) was recorded using the following parameters: modulation time 0.05 s, interval time 0.5 s, step potential 5.1 mV, modulation amplitude 25 mV. Before each DPV scan was obtained, the electrode was pretreated by scanning from 0-1 V thirty times in 0.1 M PBS until the background current response was approximately stable.

The electrode was then introduced to the phenolic solution for 300 s, at which point the scan was obtained. Background subtraction was performed in Origin 2017 software using a polynomial line shape.

To investigate the effect of waiting time on observed current density, 10 μM solutions of each phenol were prepared and the working electrode was immersed in the phenol solution. A stopwatch was used to measure the time for which the electrode was in contact with solution before voltammetry was carried out. At the desired time interval, a linear sweep voltammetry (LSV) scan was obtained at a scan rate of 50 mV s^{-1} . Once complete, the electrode was removed immediately and rinsed with deionised water. It was then scanned in PBS five times to ensure that there were no peaks remaining due to adsorbed species. This procedure was repeated for a range of time intervals and duplicated with the same electrode. Triplicates could not be obtained as the electrode performance was greatly reduced after ten uses.

Calibration curves measured by LSV were performed using a single electrode and all measurements were made in duplicate. Calibration curves measured by DPV were performed with a 300 s waiting time prior to start of scan and a newly prepared electrode was used for each measurement. All measurements were made in duplicate. Limits of detection were estimated from single measurements by quantifying the signal for the measurement and the noise level and using $S/N=3$. Analytically valid LODs were calculated from the calibration curve regression line by $3 \times \text{standard deviation of the regression line}$ divided by the slope of the regression line.

3 Results and discussion

3.1 Electrode characterisation

The bare GCE and CB-modified GCE were characterised by CV. The double-layer capacitance of bare GCE and CB-modified GCE was calculated from CV scans at scan rates between 10 and 100 mV s^{-1} (Figure 2a). A 35-fold increase in capacitance was observed upon modification of the electrode from 16 $\mu\text{F cm}^{-2}$ at the bare GCE to 560 $\mu\text{F cm}^{-2}$ at CB-GCE, reflecting the increased surface area and porosity of the CB layer.

A standard redox couple $[\text{Fe}(\text{CN})_6]^{3-/4-}$ was then used to investigate the electron transfer kinetics at both electrodes (Figure 2b). There was no change in peak separation (ΔE_p), and no shift in peak potential for the redox reaction upon modification of the electrode. The reaction was reversible at both electrodes, with ΔE_p close to 59 mV at all scan rates between 10 and 100 mV s^{-1} . A 90% increase in peak height was observed at CB-GCE compared to bare GCE, indicating an increased surface roughness of the modified electrode.

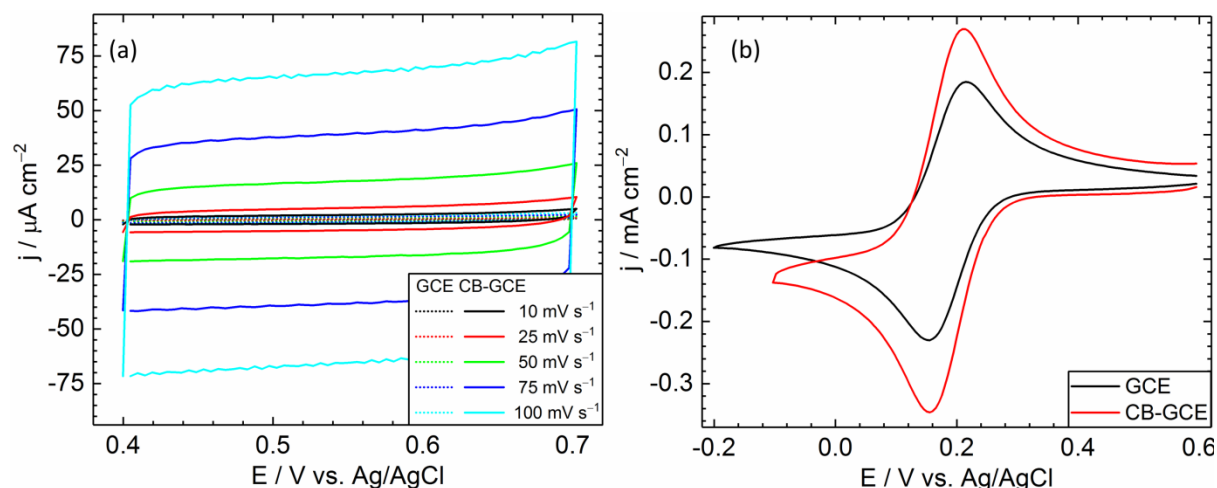


Figure 2: (a) CV scans of GCE (dotted lines) and CB-GCE (solid lines) in 0.1 M pH 7 PBS at various scan rates: 10 mV s^{-1} (black); 25 mV s^{-1} (red); 50 mV s^{-1} (green); 75 mV s^{-1} (dark blue); 100 mV s^{-1} (light blue). (b) CVs of 2 mM $[\text{Fe}(\text{CN})_6]^{3-}$ in 0.1 M pH 7 PBS at bare GCE (black) and CB-GCE (red). Scan rate 25 mV s^{-1} .

3.2 Cyclic voltammetry of phenols

Initial evaluation of the feasibility of CB modification in phenol detection was performed by CV with phenol concentration at 10 μM . Of the three phenolic compounds investigated here, catechol exhibits the most reversibility and a clearly resolved reduction peak (Figure 3a). The ET kinetics of catechol at bare GCE were slow, and ΔE_p was found to be 241 mV at scan rate 50 mV s^{-1} . Upon modification with CB, the current response improved dramatically: ΔE_p decreased to 14 mV, $E_{p(\text{OX})}$ shifted to less negative potential by 146 mV, and a 4-fold increase in j_p was observed. The reduction peak became similar in magnitude to the oxidation peak, whereas at the bare GCE it was considerable smaller compared to the oxidation peak.

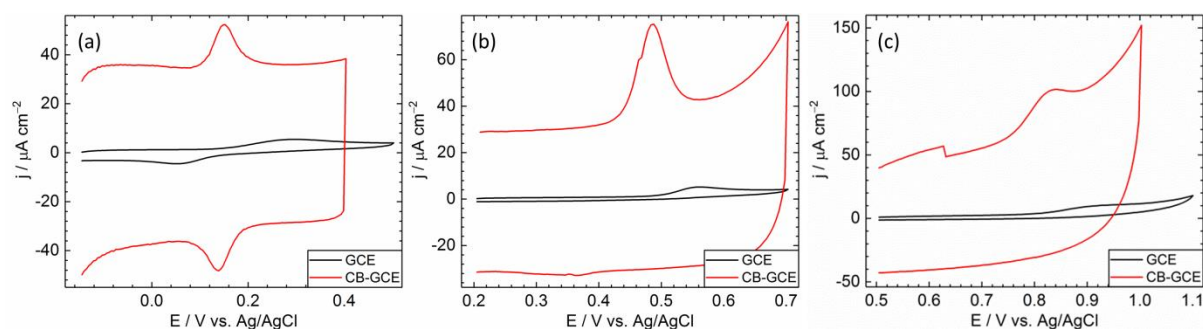


Figure 3: CV scans of 10 μM (a) catechol, (b) p-cresol and (c) p-nitrophenol at bare GCE (black lines) and CB-modified GCE (red lines). Electrolyte: 0.1 M pH 7 PBS. Scan rate: 50 mV s^{-1} .

p-Cresol manifested virtually irreversible oxidation at both electrodes (Figure 3b), but upon modification of the electrode with CB, significant improvement was observed in the current response. $E_{p(\text{OX})}$ shifted to less negative potential by 69 mV and j_p increased by an order of magnitude.

CVs of p-nitrophenol showed no trace of reduction peak (Figure 3c). The oxidation peak was poorly resolved and more of a shoulder than a peak at GCE. Again, upon modification with CB $E_{p(\text{OX})}$ shifted to less negative potential by 73 mV, and j_p increased 5-fold.

While the bare GC response is clearly diffusion-controlled, the small ΔE_p of catechol and symmetrical peak shapes of catechol and p-cresol at CB-modified electrode seem to suggest adsorbed species may be responsible for the observed peaks. This was investigated further by CV at different scan rates using 10 μ M solution of catechol. However, the oxidation peak heights were linearly dependent on the square root of scan rate (see Figure S1 in Supporting Information), confirming that the oxidation peaks are due to solution-phase species and that the symmetrical peak shapes and small ΔE_p are caused by a thin-layer effect at the porous carbon black film rather than adsorption.

3.3 Time dependence of phenol oxidation current density

Current magnitude at CB-GCE was found to be strongly dependent on waiting time prior to start of potential sweep, and further current enhancement was observed when the electrode was allowed to stand in solution for longer. LSV was performed with waiting times between 10 and 90 seconds at both bare GCE and CB-GCE. The extent of enhancement varied with the identity of the phenolic compound. The smallest enhancement was seen for catechol, where oxidation peak height increased by 20% (Figure 4b). For p-cresol, a 60% enhancement was observed (Figure 4d), and for p-nitrophenol the peak height increased 4-fold when waiting time was increased from 10 s to 90 s (Figure 4f). At the bare GCE no trend of enhancement with waiting time was seen for either catechol (Figure 4a) or p-cresol (Figure 4c), and only ca. 2% enhancement was observed in the case of p-nitrophenol (Figure 4e). These experiments demonstrate that a large current increase can be obtained by using CB-modified electrodes, and even short waiting times can lead to greatly improved current responses.

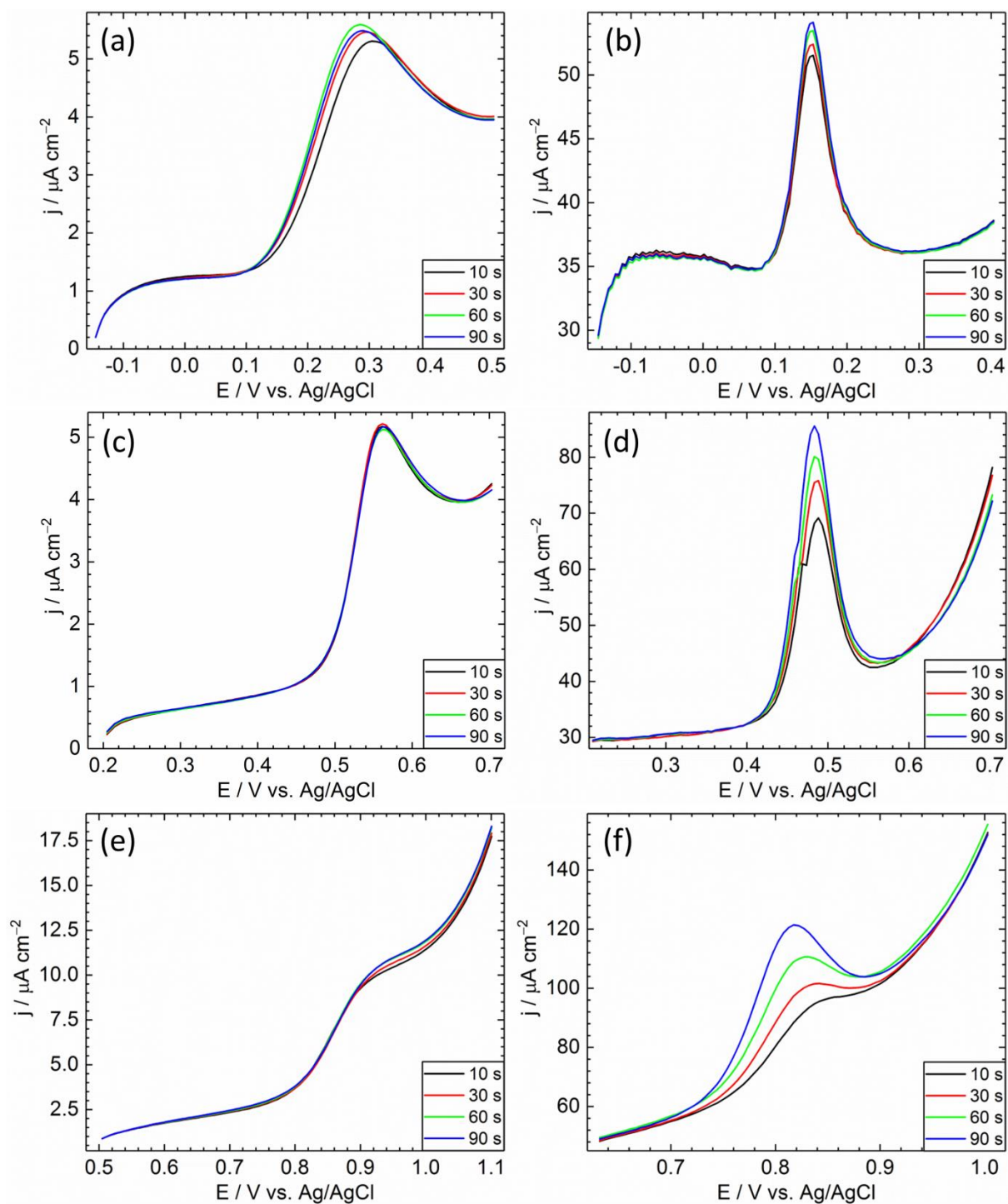


Figure 4: LSV scans of 10 μM catechol (a, b); 10 μM p-cresol (c, d); 10 μM p-nitrophenol (e, f) at GCE (a, c, e) and CB-GCE (b, d, f) after various waiting times with working electrode immersed in catechol solution: 10 s (black); 30 s (red); 60 s (green); 90 s (blue). Electrolyte: 0.1 M pH 7 PBS. Scan rate 50 mV s^{-1} .

3.4 Detection in nM range

DPV was employed to determine the ability of both bare GCE and CB-modified GCE to detect each phenolic compound at nM range, and 300 s waiting time was included prior to recording the DPVs to enhance the detection ability. Background subtraction was performed to quantify the peak current densities (Figure 5). To allow comparison between the two different electrodes, rough estimates of the limit of detection were calculated from single measurements based on $S/N=3$.

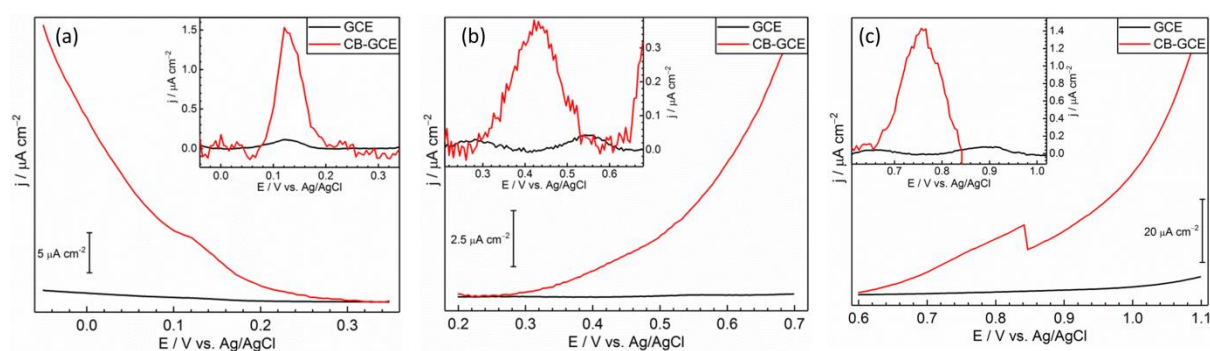


Figure 5: DPV scans of (a) 50 nM catechol; (b) 100 nM p-cresol and (c) 500 nM p-nitrophenol at bare GCE (black lines) and CB-modified GCE (red lines). The curves have been offset in the y direction for clarity. Insets: DPV curves in main figures after background subtraction. Electrolyte: 0.1 M pH 7 PBS. The sudden current drop at ca. 0.82 V vs. Ag/AgCl in (c) is due to the potentiostat and can be ignored.

Figure 5a shows DPVs of 50 nM catechol as recorded (main figure) and after background subtraction (inset). The peak current density at CB-GCE is over an order of magnitude greater than at the bare GCE. LOD is estimated to be 5 nM at CB-GCE and 10 nM at GCE. In Figure 5b DPVs of 100 nM p-cresol are compared. Again, modifying the electrode with CB enhances the peak current density 10-fold, and LOD is estimated at 16 and 63 nM at CB-GCE and GCE, respectively. In the case of 500 nM p-nitrophenol (Figure 5c) the peak

current density was 18 times greater at CB-GCE compared to GCE. Limits of detection were estimated at 55 and 154 nM at CB-GCE and GCE, respectively.

3.5 Calibration curves for catechol and p-cresol

LSV and DPV were used to construct calibration curves of catechol using CB-modified electrodes (Figure 6). At concentrations between 1 and 10 μM LSV offers adequate sensitivity of $2.4 \mu\text{A cm}^{-2} \mu\text{M}^{-1}$ and excellent linear response with small associated error in the measurements. This also demonstrates that measurements with a single electrode are highly reproducible when performed in low concentration of phenol, although long-term use will be impeded by electrode fouling. DPV gives good linear response in concentration range 100 nM to 5 μM and impressive sensitivity of $23 \mu\text{A cm}^{-2} \mu\text{M}^{-1}$. DPV scans, each recorded using a freshly prepared electrode, show the reproducibility of the electrode preparation method. Detection limits were also calculated from the regression lines and they were found to be 79 nM (LSV, Figure 6a) and 41 nM (DPV, Figure 6b).

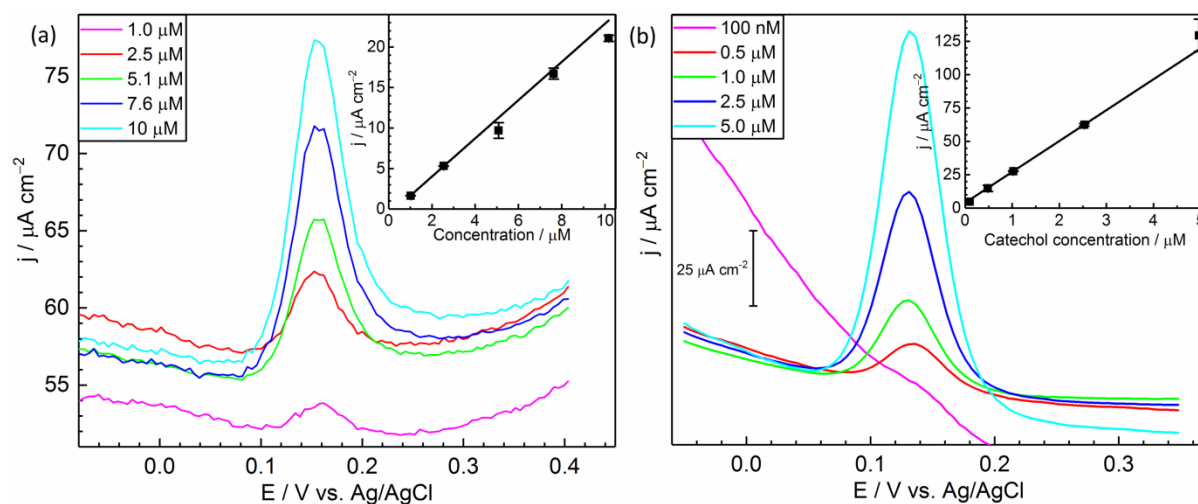


Figure 6: (a) LSVs at scan rate 50 mV s^{-1} and (b) DPVs of catechol at various concentrations at CB-GCE. DPV curves have been offset in the y direction for clarity. Inset: Peak height of current density as a function of catechol concentration. Electrolyte: 0.1 M pH 7 PBS.

A calibration curve was also constructed for p-cresol at CB-GCE using LSV (Figure 7). Good linear response was obtained in concentration range 1-10 μM with good reproducibility of measurements. The sensitivity of this method was found to be $2.7 \mu\text{A cm}^{-2} \mu\text{M}^{-1}$, and LOD calculated from the regression line was found to be 63 nM.

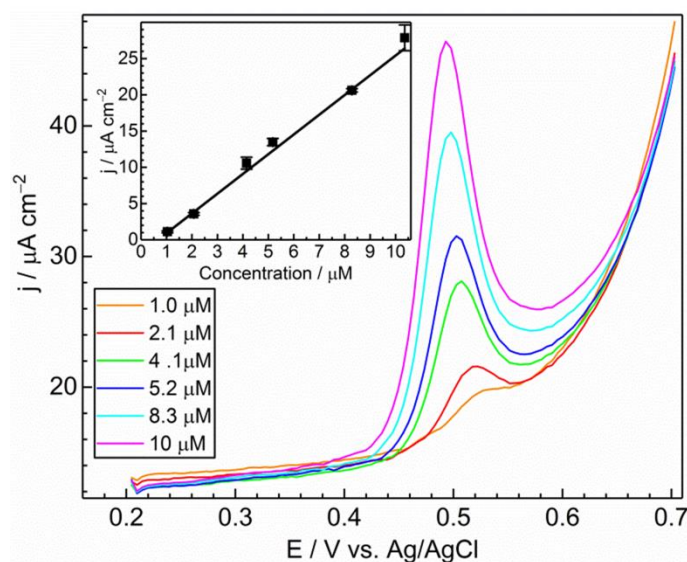


Figure 7: LSV scans of various concentrations of p-cresol at CB-modified GCE. Scan rate 50 mV s^{-1} . Inset: peak current density as a function of p-cresol concentration.

Several electrochemical sensors have been reported for catechol and p-cresol detection. For example, a reduced graphene oxide-MWCNT p-cresol sensor was reported [25], which had a sensitivity of $5.7 \mu\text{A cm}^{-2} \mu\text{M}^{-1}$ and LOD $1.6 \mu\text{M}$. A SWCNT-based sensor showed better sensitivity towards p-cresol ($95 \mu\text{A cm}^{-2} \mu\text{M}^{-1}$) and a lower LOD (3.7 nM) [20]. In the same study catechol was detected with a sensitivity of $135 \mu\text{A cm}^{-2} \mu\text{M}^{-1}$ and LOD 2.3 nM . A carbon nanocage-reduced graphene oxide sensor for catechol demonstrated a sensitivity of $0.21 \mu\text{A cm}^{-2} \mu\text{M}^{-1}$ and LOD 400 nM [19]. Carbon black has also been reported as electrochemical sensor towards catechol before, when it was used to modify a screen-printed electrode: sensitivity of $18 \mu\text{A cm}^{-2} \mu\text{M}^{-1}$ and LOD 100 nM were obtained [23]. In

comparison, the carbon black modified electrochemical sensor presented in this study demonstrates a better performance than many of the more expensive carbon nanomaterials.

Table 1: Comparisons of the analytical performance of various carbon nanomaterial-based sensors in DPV detection of p-cresol and catechol. GO=graphene oxide; MWCNT=multiwalled carbon nanotube; SWCNT=singlewalled carbon nanotube; CNC=carbon nanocage; RGO=reduced graphene oxide.

Sensor	Analyte	Sensitivity / $\mu\text{A cm}^{-2} \mu\text{M}^{-1}$	LOD / nM	Ref.
GO-MWCNT	p-Cresol	5.7	1600	[25]
SWCNT	p-Cresol	95	3.7	[20]
CB	p-Cresol	2.7	63	This work
SWCNT	Catechol	135	2.3	[20]
CNC-RGO	Catechol	0.21	400	[19]
CB	Catechol	23	41	This work

4 Conclusion

Carbon black, a low-cost carbon nanomaterial that is readily available in bulk quantities, was used in electrochemical detection of phenolic compounds catechol, p-cresol and p-nitrophenol by dropcoating onto a glassy carbon electrode. Compared to bare GCE, at CB-GCE higher current density is observed, and oxidation potentials move to less positive potential for all three phenolic compounds studied. Calibration curves were constructed for catechol and p-cresol, demonstrating good linear response to both phenolic compounds in the low μM range, excellent sensitivity and limits of detection in nM. As electrochemical sensor,

carbon black is shown to be competitive compared with other, more expensive carbon nanomaterials.

References

1. Karim, F.; Fakhruddin, A. N. M., Recent advances in the development of biosensor for phenol: a review. *Reviews in Environmental Science and Bio/Technology* **2012**, *11* (3), 261-74. DOI: <http://dx.doi.org/10.1007/s11157-012-9268-9>
2. Alam, M. K.; Rahman, M. M.; Abbas, M.; Torati, S. R.; Asiri, A. M.; Kim, D.; Kim, C., Ultra-sensitive 2-nitrophenol detection based on reduced graphene oxide/ZnO nanocomposites. *Journal of Electroanalytical Chemistry* **2017**, *788*, 66-73. DOI: <http://dx.doi.org/10.1016/j.jelechem.2017.02.004>
3. Michałowicz, J.; Duda, W., Phenols – Sources and Toxicity. *Polish Journal of Environmental Studies* **2007**, *16* (3), 347-62.
4. Ahel, M.; McEvoy, J.; Giger, W., Bioaccumulation of the lipophilic metabolites of nonionic surfactants in freshwater organisms. *Environmental Pollution* **1993**, *79* (3), 243-8. DOI: [http://dx.doi.org/10.1016/0269-7491\(93\)90096-7](http://dx.doi.org/10.1016/0269-7491(93)90096-7)
5. Mayer, T.; Bennie, D.; Rosa, F.; Rekas, G.; Palabrica, V.; Schachtschneider, J., Occurrence of alkylphenolic substances in a Great Lakes coastal marsh, Cootes Paradise, ON, Canada. *Environmental Pollution* **2007**, *147* (3), 683-90. DOI: <http://dx.doi.org/10.1016/j.envpol.2006.09.012>
6. Liu, J.; Wang, R.; Huang, B.; Lin, C.; Wang, Y.; Pan, X., Distribution and bioaccumulation of steroidal and phenolic endocrine disrupting chemicals in wild fish species from Dianchi Lake, China. *Environmental Pollution* **2011**, *159* (10), 2815-22. DOI: <http://dx.doi.org/10.1016/j.envpol.2011.05.013>

7. Lee, C.-C.; Jiang, L.-Y.; Kuo, Y.-L.; Chen, C.-Y.; Hsieh, C.-Y.; Hung, C.-F.; Tien, C.-J., Characteristics of nonylphenol and bisphenol A accumulation by fish and implications for ecological and human health. *Science of The Total Environment* **2015**, 502, 417-25. DOI: <http://dx.doi.org/10.1016/j.scitotenv.2014.09.042>
8. Bureau, E. C. *European Union Risk Assessment Report: Phenol*; 2006.
9. Agency, U. S. E. P. *Phenol Fact Sheet*; 2000.
10. Hu, C.; Chen, B.; He, M.; Hu, B., Amino modified multi-walled carbon nanotubes/polydimethylsiloxane coated stir bar sorptive extraction coupled to high performance liquid chromatography-ultraviolet detection for the determination of phenols in environmental samples. *Journal of Chromatography A* **2013**, 1300, 165-72. DOI: <http://dx.doi.org/10.1016/j.chroma.2013.05.004>
11. Yang, Y.; Lu, L.; Zhang, J.; Yang, Y.; Wu, Y.; Shao, B., Simultaneous determination of seven bisphenols in environmental water and solid samples by liquid chromatography–electrospray tandem mass spectrometry. *Journal of Chromatography A* **2014**, 1328, 26-34. DOI: <http://dx.doi.org/10.1016/j.chroma.2013.12.074>
12. Azzouz, A.; Ballesteros, E., Trace analysis of endocrine disrupting compounds in environmental water samples by use of solid-phase extraction and gas chromatography with mass spectrometry detection. *Journal of Chromatography A* **2014**, 1360, 248-57. DOI: <http://dx.doi.org/10.1016/j.chroma.2014.07.059>
13. Gong, S.-X.; Wang, X.; Chen, Y.; Cheng, C.-G.; Wang, M.-L.; Zhao, R.-S., Carboxylated solid carbon spheres as a novel solid-phase microextraction coating for sensitive determination of phenols in environmental water samples. *Journal of Chromatography A* **2015**, 1401, 17-23. DOI: <http://dx.doi.org/10.1016/j.chroma.2015.04.056>
14. Sarafraz-Yazdi, A.; Dizavandi, Z. R.; Amiri, A., Determination of phenolic compounds in water and urine samples using solid-phase microextraction based on sol-gel technique

prior to GC-FID. *Analytical Methods* **2012**, 4 (12), 4316-25. DOI:

<http://dx.doi.org/10.1039/C2AY25970B>

15. Perez Lopez, B.; Merkoci, A., Improvement of the electrochemical detection of catechol by the use of a carbon nanotube based biosensor. *Analyst* **2009**, 134 (1), 60-4. DOI: 10.1039/B808387H
16. Lete, C.; Lupu, S.; Marin, M.; Badea, M., New composite materials used in the phenol electroanalysis. Part i. Poly(azulene)/prussian blue and prussian blue/poly(azulene) films. *Revue Roumaine de Chimie* **2010**, 55 (6), 335-40.
17. Stradiotto, N. R.; Yamanaka, H.; Zandoni, M. V. B., Electrochemical Sensors: A Powerful Tool in Analytical Chemistry. *Journal of the Brazilian Chemical Society* **2003**, 14 (2), 159-73. DOI: <http://dx.doi.org/10.1590/S0103-50532003000200003>
18. Shah, B.; Lafleur, T.; Chen, A., Carbon nanotube based electrochemical sensor for the sensitive detection of valacyclovir. *Faraday Discussions* **2013**, 164 (0), 135-46. DOI: 10.1039/C3FD00023K
19. Huang, Y. H.; Chen, J. H.; Sun, X.; Su, Z. B.; Xing, H. T.; Hu, S. R.; Weng, W.; Guo, H. X.; Wu, W. B.; He, Y. S., One-pot hydrothermal synthesis carbon nanocages-reduced graphene oxide composites for simultaneous electrochemical detection of catechol and hydroquinone. *Sensors and Actuators B: Chemical* **2015**, 212, 165-73. DOI: <http://dx.doi.org/10.1016/j.snb.2015.02.013>
20. Govindhan, M.; Lafleur, T.; Adhikari, B.-R.; Chen, A., Electrochemical Sensor Based on Carbon Nanotubes for the Simultaneous Detection of Phenolic Pollutants. *Electroanalysis* **2015**, 27 (4), 902-9. DOI: <http://dx.doi.org/10.1002/elan.201400608>
21. Yang, L.; Fan, S.; Deng, G.; Li, Y.; Ran, X.; Zhao, H.; Li, C.-P., Bridged β -cyclodextrin-functionalized MWCNT with higher supramolecular recognition capability: The

- simultaneous electrochemical determination of three phenols. *Biosensors and Bioelectronics* **2015**, 68, 617-25. DOI: <http://dx.doi.org/10.1016/j.bios.2015.01.059>
22. Rahman, M. M.; Balkhoyor, H. B.; Asiri, A. M., Phenolic sensor development based on chromium oxide-decorated carbon nanotubes for environmental safety. *Journal of Environmental Management* **2017**, 188, 228-37. DOI: <http://dx.doi.org/10.1016/j.jenvman.2016.12.008>
23. Talarico, D.; Arduini, F.; Constantino, A.; Del Carlo, M.; Compagnone, D.; Moscone, D.; Palleschi, G., Carbon black as successful screen-printed electrode modifier for phenolic compound detection. *Electrochemistry Communications* **2015**, 60, 78-82. DOI: <http://dx.doi.org/10.1016/j.elecom.2015.08.010>
24. Compagnone, D.; Carlo, M. D.; Innocenzi, D.; Arduini, F.; Agüí, L.; Serafín, V. In *Carbon Black modified glassy carbon electrode for the detection of antioxidants compounds*, 2015 XVIII AISEM Annual Conference, 3-5 Feb. 2015; 2015; pp 1-3.
25. Hu, F.; Chen, S.; Wang, C.; Yuan, R.; Yuan, D.; Wang, C., Study on the application of reduced graphene oxide and multiwall carbon nanotubes hybrid materials for simultaneous determination of catechol, hydroquinone, p-cresol and nitrite. *Analytica Chimica Acta* **2012**, 724, 40-6. DOI: <http://dx.doi.org/10.1016/j.aca.2012.02.037>